pH-Responsive Poly(Ethylene Glycol)-*block*-Polylactide Micelles for Tumor-Targeted Drug Delivery

Lin Xiao, [†,‡] *Lixia Huang,* [†,‡] *Firmin Moingeon,* [§] *Mario Gauthier,* [§,*] *Guang Yang*[†,*]

[†] Department of Biomedical Engineering, College of Life Science and Technology, Huazhong University of Science and Technology, Wuhan 430074, China.

[§] Department of Chemistry, University of Waterloo, Waterloo N2L 3G1, Canada.

KEYWORDS: pH-responsive, copolymer, micelles, drug delivery, tumor targeting

ABSTRACT: A biodegradable micellar drug delivery system with a pH-responsive sheddable PEG shell was developed using an acetal-linked poly(ethylene glycol)-*block*-polylactide (PEG-*a*-PLA) copolymer and applied to the tumoral release of paclitaxel (PTX). The micelles with a diameter of ca. 100 nm were stable in PBS at pH 7.4, started shedding the shell and aggregating slowly at pH 6.5, and decomposed faster at pH 5.5. PTX-loaded micelles (M-PTX) with a drug loading of 6.9 wt% exhibited pH-triggered PTX release in simulated tumoral acidic environments corresponding to the extracellular and intracellular spaces. *In vitro* experiments showed that the micelles were non-cytotoxic to different cell lines, while M-PTX inhibited the proliferation and promoted the apoptosis of Hela cells. An *in vivo* study with Hela tumor-bearing mice indicated

that M-PTX efficiently inhibited tumor growth. Due to these properties, the PEG-*a*-PLA micellar system appears to have bright prospects as a tumor-targeting drug carrier.

1. INTRODUCTION

Nonspecific interactions between foreign materials and serum components *in vivo* is one of the main challenges for drug delivery systems used in cancer therapy, as it can lead to extensive aggregation and the rapid clearance of nanoparticles from circulation by the immune system.[1] To overcome this challenge, a variety of hydrophilic polymers with stealth behavior have been developed to modify and stabilize drug delivery systems, among which poly(ethylene glycol) (PEG) is the most commonly applied non-ionic polymer because of its superior biocompatibility and water solubility.[2-4] It is widely accepted that PEGylation is highly effective to minimize nonspecific interactions and to prolong the circulation time of nanoparticles *in vivo* since the 1990s.[5-10] Unfortunately, recent studies also indicated that PEGylation may significantly reduce nanoparticle uptake by tumor cells, leading to greatly reduced therapeutic efficacy.[11, 12] It has been suggested that the cleavage of PEG chains from nanoparticles could facilitate cellular uptake.[13-15] It was thus proposed that an ideal drug delivery system for cancer therapy should be colloidally stable in circulation, with a protective layer such as a shell of PEG chains, but allow shedding of the shell at the tumor site to promote cellular internalization.[16-17] Shedding of the shell was also accompanied by dissociation of the particles in some cases, thus leading to more efficient drug release.[18] The unique features of tumor tissues such as intracellular reduction, mild acidity, and the presence of specific proteins can be employed as triggers to induce PEG shedding from nanoparticles through appropriate material design.[19-32] Zhong and coworkers [19-22] thus developed a series of reduction-sensitive micelles with a sheddable shell for tumor-targeted

drug delivery based on disulfide-linked block copolymers. The disulfide bonds cleaved in response to the reductive environment in tumor cells, leading to rapid release of the drug. The *in vivo* performance demonstrated that these reduction-sensitive systems achieved significantly enhanced therapeutic efficacy and minimal side effects. The existence of a pH gradient between tumor tissues and the blood has also been considered an effective trigger to increase cell uptake and/or for the selective release of drugs in tumor tissues.[23-29] For example, Meier et al.[25] prepared a series of pH-responsive micelles from poly(dimethysiloxane)-*block*-poly(2-(dimethylamino)ethyl methacrylate) for intracellular anticancer drug delivery. The carriers released doxorubicin in response to a decrease in pH from 7.4 to 5.5. Meng and coworkers[28] reported pH-sensitive degradable polymersomes based on poly(ethylene glycol)-*block*-poly(2,4,6-trimethoxybenzylidenepentaerythritol carbonate) for the controlled release of PTX and doxorubicin hydrochloride. Kataoka et al.[29] prepared pH-sensitive polyion complex micelles from lactosylated PEG-siRNA conjugates and polyethylenimine (PEI) for siRNA delivery.

While different nanoparticle systems with controlled shell-shedding and triggered drug release mechanisms have been developed for tumor treatment, their shell-shedding and drug release characteristics in the extracellular and intracellular spaces were not compared, especially for the pH-responsive systems, which limits the understanding of the behavior of these nanoparticles *in vivo* to some extent. In this work, a simple pH-sensitive micellar system with a sheddable shell was designed for tumor-targeted drug delivery based on block copolymers of PEG and PLA with an acid-labile acetal group (PEG-*a*-PLA; Scheme 1). Shedding of the PEG chains and drug release triggered by tumoral acidic conditions characteristic for both the extracellular and intracellular spaces were demonstrated. Furthermore, enhanced antitumor efficacy was achieved *in vitro* using the PTX-loaded pH-sensitive micelles (M-PTX) as compared with both their non-

responsive counterpart and the free drug. It is well-known that good biocompatibility and biodegradability are important properties for drug delivery vehicles, and both PEG and PLA have been approved for biological use by the FDA.[33-36] This efficient and safe micellar system therefore appears to have bright prospects in tumor treatment.

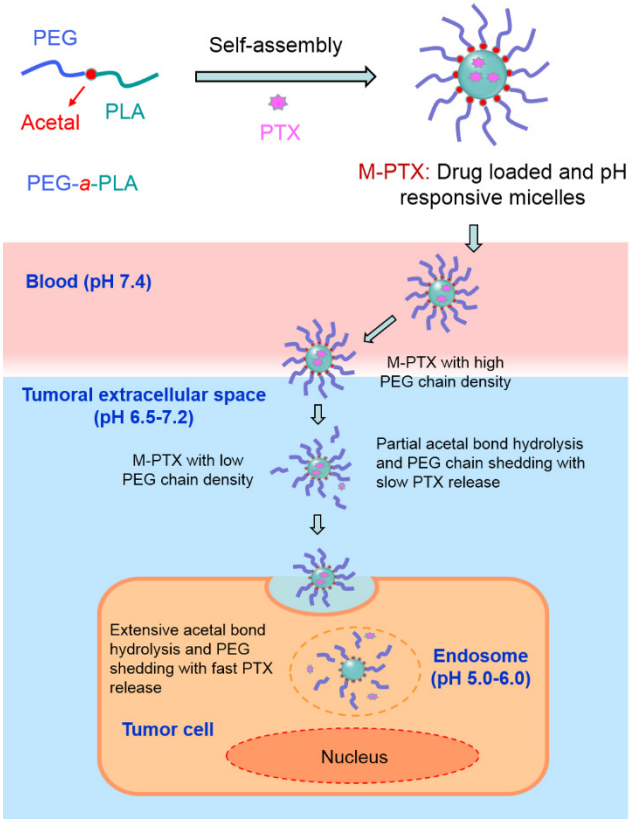

Scheme 1. Illustration of M-PTX preparation, pH-triggered PEG shell shedding and drug release in response to tumoral acidity in the extracellular and intracellular spaces.

2. EXPERIMENTAL SECTION

2.1 Materials, Cell lines and Animals

All the chemicals employed in the procedures were purchased from Sigma-Aldrich and used as received unless otherwise noted. The lactide was recrystallized three times from dry ethyl

acetate, dried under vacuum, and stored at -20 ℃ until further use. The $Sn(Oct)_2$ catalyst was first purified by distillation under reduced pressure and stored under nitrogen. The antitumor drug PTX and the fluorescent dye coumarin-6 (C6) were purchased from Aladdin Co. (Shanghai, China). Cell counting kits (CCK-8), DPAI and FITC were purchased from Dojindo Co. (Shanghai, China).

The Hela cell line, human non-tumor hepatic cell line (L-02), and human umbilical vein endothelial cell line (HUVEC) were used in this study. The information on their source, culture and incubation conditions is given in the Supporting Information.

Nude female Balb/c mice (4 weeks old, body weight: 16± 2 g) were purchased from Charles River Co. (Beijing, China). All the animal procedures were performed according to the research protocol approved by the Animal Experimentation Ethics Committee of Huazhong University of Science and Technology.

2.2 Synthesis and characterization of PEG-*a*-PLA copolymer

The method for the synthesis of the PEG-*a*-PLA block copolymer was developed by adapting a procedure reported by Hashimoto et al.[37] for the synthesis of polyurethanes with degradable acetal linkages. A block copolymer with a non-cleavable block junction (PEG-*b*-PLA) was also synthesized. Gel permeation chromatography (GPC) and ^1H NMR were employed to characterize the copolymers. The detailed synthetic procedures and characterization methods used are provided in the Supporting Information.

2.3 Preparation, properties and characterization of PEG-*a*-PLA micelles

Preparation of PEG-a-PLA micelles

PEG-*a*-PLA micelles were prepared as follows: A 1.0 wt % solution of PEG-*a*-PLA in N, N-dimethylformamide (DMF) was prepared (typically 10 mg of copolymer in 1 g of DMF). Deionized water was added drop-wise to the solution with vigorous stirring at a rate of 1 mL/h, until a water content of 50 wt% was reached. The aggregates formed were then quenched by slowly adding the slightly turbid solution to 8 g of deionized water to freeze their morphology. The solution was subsequently dialyzed against deionized water for 3 days to remove all solvent residues. The concentration of the final solution was ca. 1.0 mg/mL.

Self-assembly behavior investigation

^{1}H NMR analysis was employed to confirm the self-assembly of PEG-*a*-PLA. The critical micelle concentration (CMC) was measured by a fluorescence method using pyrene as a probe. Detailed protocols for these experiments can be found in the Supporting Information.

Effects of heat treatment on the size distribution of PEG-a-PLA micelles

A thermal treatment was employed to obtain micelles with a narrower size distribution. Briefly, a 1.0 wt % solution of PEG-*a*-PLA in DMF was first prepared. Deionized water was added drop-wise to the solution with vigorous stirring at a rate of 1 mL/h, until a water content of 10 wt% (100 μL) was reached. A 100 μL sample was withdrawn and the slightly turbid solution was heated to 60 ℃ with vigorous stirring for 10 min, until it became transparent. Then another 100 μL aliquot of deionized water was added drop-wise at room temperature with vigorous stirring at a rate of 1 mL/h, to obtain a slightly turbid solution, at which point a second 100 μL sample was withdrawn, followed by a second heat treatment by the same procedure. Third and fourth samples were also withdrawn in that manner. All the samples were subjected to size distribution analysis by dynamic light scattering (DLS).

pH responsiveness of PEG-a-PLA micelles

The size change of micelles in response to pH was monitored by DLS measurements. Briefly, micelles were subjected to treatments at pH 7.4, 6.5 and 5.5 in PBS, respectively, at 37 ℃ with a stirring speed of 200 rpm. At different time intervals, the size was determined by DLS. Size changes were also monitored for micelles incubated in the cell culture medium at 37°C in the presence of 10% FBS.

Characterization

Transmission electron microscopy (TEM) was employed to characterize the morphology of the micelles, using a Hitachi H-7000FA instrument operated at 100 kV and equipped with a CCD camera. Samples were prepared by dropping 10 μL of micellar solution onto a TEM grid followed by drying in air for 24 h. The hydrodynamic size of the micelles was determined at 0.025 wt% concentration by DLS analysis on a Malvern Zetasizer Nano ZS90 (Malvern Instruments, Ltd., U.K.) equipped with a 4 mW He–Ne laser source (λ = 633 nm, scattering angle 90°). The micellar solutions were filtered through a 0.45 μm Millipore filter prior to analysis.

2.4 Drug loading and simulated release *in vitro*

Preparation and characterization of drug-loaded micelles

PTX-loaded PEG-*a*-PLA micelles (M-PTX) were prepared by mixed self-assembly of the copolymer and PTX using a procedure similar to the preparation of the PEG-*a*-PLA micelles. Briefly, the copolymer (10 mg) and PTX (1 mg) were first dissolved in 1 g of DMF, followed by cycles of water addition, quenching and dialysis as described in Section 2.3. The concentration

of the final solution was ca. 1.0 mg/mL. PTX-loaded PEG-*b*-PLA micelles (M_b-PTX) were prepared by the same method, to be used as a control in the subsequent studies.

The entrapment efficiency (EE%) and drug loading capacity (DLC%) were determined by HPLC after dissolving M-PTX in acetonitrile.[38] The HPLC system used consisted of a C-18 column (4.6 mm × 250 mm) with 5 μm packing (Agilent Instruments, USA). The mobile phase was a mixture of acetonitrile and water in a ratio of 55:45 (v/v), at a flow rate of 1 mL/min. The sample (100 μL) was injected with an autoinjector (Agilent Instruments, USA), and the paclitaxel content was quantified by UV detection (227 nm, Agilent Instruments, USA). A calibration curve for paclitaxel was prepared in acetonitrile and used to determine the paclitaxel concentration. The EE% and DLC% were calculated using Equations (1) and (2), respectively.

$$\text{Entrapment Efficiency (EE\%)} = \frac{Weight\,of\ drug\,in\,micelles}{Weight\,of\ drug\,in\ feed} \times 100\% \qquad (1)$$

$$\text{Drug Loading Capacity (DLC\%)} = \frac{Weight\,of\ drug\,in\,micelles}{Weight\,of\ drug\text{-}loaded\,micelles} \times 100\% \qquad (2)$$

pH-triggered release of PTX from M-PTX

To simulate drug release in human blood and in the tumoral sites (both extracellular and intracellular spaces) *in vitro*, release profiles of PTX from M-PTX were obtained in PBS at pH 7.4, 6.5 and 5.5, respectively, in the presence of 1 M sodium salicylate, by a dialysis method.[39] Sodium salicylate was used to achieve good sink conditions for PTX, as it can increase the aqueous solubility of PTX remarkably.[40] Briefly, 1 mL of M-PTX solution was introduced into a dialysis tube (MWCO 3500) and dialyzed against 50 mL of PBS containing 1 M sodium salicylate at 37 ℃ with stirring at 100 rpm for 72 h. At preset time intervals (0, 1, 2, 4, 6, 8, 12,

16, 20, 24, 36, 48, 60, 72 h), 1 mL of the dialysis medium was withdrawn and an equal volume of fresh medium was added. The PTX release profiles from M*b*-PTX and for free PTX under the same conditions were also studied as controls. The samples were analyzed by HPLC under the conditions described above.

2.5 Cytotoxicity and cellular internalization of PEG-*a*-PLA micelles

Cytotoxicity of PEG-a-PLA micelles

The cytotoxicity of the PEG-*a*-PLA micelles was evaluated using the CCK-8 assay with Hela cells, L-02 cells, and HUVEC, respectively. Briefly, Hela cells and L-02 cells (1×10^4/well) were cultured in 96-well plates and incubated overnight. PEG-*a*-PLA micellar solution was then added to each well at different concentrations before incubation for 24, 48 and 72 h, respectively. For HUVEC, the cells were seeded at 5×10^3/well in 96-well plates and incubated overnight. PEG-*a*-PLA micellar solution was then added to each well at different concentrations before incubation for 24, 72 and 120 h, respectively. This modified procedure was used because HUVEC cells are larger and proliferate more slowly than the two other cell lines. Then 10 μL of CCK-8 was added to each well. After incubation for 30 min at 37 ℃ in a humidified atmosphere containing 5% CO_2, the absorbance was measured at 450 nm using a microplate reader (Thermo Fisher, USA). The cell viability was calculated using Equation (3) where OD_S, OD_B and OD_N are the OD values for the samples, blank control and negative control, respectively.

$$\text{Cell viability} = \frac{OD_S - OD_B}{OD_N - OD_B} \times 100\% \qquad (3)$$

Cellular internalization of PEG-a-PLA micelles

To study the cellular internalization of PEG-*a*-PLA micelles, coumarin-6 labeled micelles (M-C6) were prepared by mixed self-assembly of the copolymer and C6 through procedures similar to those described for M-PTX in Section 2.4. To mimic the extracellular environment of tumor tissues, M-C6 samples were subjected to treatment with PBS at pH 6.5 for different time periods before use. Hela cells (5×10^4/well) were seeded on 8-chamber slides (Lab Tek Ⅱ, Thermo Fisher) and incubated overnight. Then the pretreated M-C6 (0.2 mg/mL) were incubated with the cells for 30 min. After removing the M-C6-containing medium the cells were washed with PBS three times, stained with DAPI for 15 min, and washed three times with PBS. The samples were imaged with a confocal laser scanning microscope (Olympus, FV1000). The cellular internalization of M-C6 without treatment, C6-loaded non-responsive PEG-*b*-PLA micelles (M_b-C6) and of free C6 were also investigated as controls.

2.6 *In vitro* antitumor assay

Cytotoxicity of M-PTX to Hela cells

Hela cells were seeded in 96-well plates at 1×10^4 cells per well and incubated at 37 ℃ overnight. Various formulations including M-PTX, M_b-PTX and free PTX were then added to the cells corresponding to different PTX concentrations. It should be noted that the pH of the culture medium was adjusted to 6.5 with 0.1 M HCl before the treatment, to mimic the extracellular environment in tumor tissues. After 48 h of incubation, the cytotoxicity of each formulation was evaluated by the CCK-8 assay as described in Section 2.5. The cytotoxicity of these PTX formulations to Hela cells was also evaluated in normal culture medium (i.e. culture medium without pH adjustment).

Cell cycle analysis

Cell cycle analysis was performed using propidium iodide (PI; Keygentec, China) staining to measure the DNA content and distribution of cells in various cell cycle phases. Hela cells (30 $\times 10^4$/well) were seeded in 6-well plates and incubated overnight, followed by treatment with M-PTX, M_b-PTX and PTX (0.1 μg /mL) for 48 h. Cells without treatment were used as control. Moreover, to mimic the extracellular environment in tumor tissues, the treatment with M-PTX and M_b-PTX was also used for Hela cells at pH 6.5 (the pH of the culture medium was adjusted to 6.5 with 0.1 M HCl before treatment). The Hela cells were harvested and suspended in cold PBS, and fixed with 90% cold ethanol at -20 ℃ overnight. The cells were then resuspended in PBS containing RNaseA (Solarbio, China) and incubated at 37 ℃ for 40 min to remove the RNA. Finally, the cells were stained with PI at 4 ℃ for 20 min in the dark. The data were calculated using the Cell Quest and Modfit software packages to determine the cell cycles.

Cellular apoptosis assay

The Hela cells were subjected to treatment with M-PTX, M_b-PTX and PTX (0.1 μg /mL) for 48 h as described above. The cells were sequentially washed, trypsinized, washed and centrifuged. Cellular apoptosis was performed on a flow cytometer (BD FACSCalibur, USA) using the Annexin V-FITC (Annexin V) and PI detection kits, according to the manufacturers' instructions.

To further study the mechanism of antitumor activity of M-PTX, the gene expression assay was performed for M-PTX-treated Hela cells. The protocol used is provided in the Supporting Information.

2.7 *In vivo* experiments

In vivo and ex vivo imaging

Subcutaneous tumors were developed in female nude mice by the subcutaneous injection of 2 $\times 10^6$/0.2 mL Hela cells in the axillary region. The mice were used for the study when the tumor grew to approximately 200 mm^3.

C6 and M-C6 were administered *via* tail vein injection at the same concentration of C6. For *in vivo* imaging 0, 6, 24 and 48 h post-injection, the tumor-bearing mice were anesthetized with isoflurane (RWD Life Science, China) and the fluorescence images were captured with a 1-s exposure time using a small animal *in vivo* fluorescence imaging system (IVIS Lumina XRMS II, PerkinElmer, USA). The mice were sacrificed at 24 and 48 h post-injection and their tumor tissues were subjected to *ex vivo* fluorescence imaging using frozen sections by confocal fluorescence microscopy (Olympus FU1000, Japan).

Anti-tumor effect

The tumor-bearing mice were randomly divided into three groups of five mice each. PTX and M-PTX were administered *via* tail vein injection at the same PTX concentration (the dose was 5 mg/kg) every 3 days over 36 days. The tumor volume and body weight of the mice were measured 3 days after each injection, immediately before the next injection. The mice were sacrificed and the tumor tissues were harvested and fixed in 4% paraformaldehyde 3 days after the last injection. For histopathological analysis, tumor paraffin sections were stained with hematoxylin and eosin (HE, Servicebio, China). Immunohistochemical staining with antibodies against proliferating cell nuclear antigen (PCNA) was done to evaluate the proliferation of tumor cells. The frozen tumor sections were used to assess apoptosis by the method of terminal deoxynucleotidyl transferase mediated dUTP nick end labeling (TUNEL).

2.8 Statistical analysis

Descriptive data are expressed as the arithmetic mean value ± standard deviation (SD). All the quantitative results were obtained from at least triplicate samples. Data on cytotoxicity of different PTX formulations were analyzed statistically using Student's t test. P values of 0.05 or less were considered significant.

3. RESULTS AND DISCUSSION

3.1 Synthesis and characterization of the PEG-*a*-PLA and PEG-*b*-PLA copolymers

The synthesis of the copolymers was achieved according to the reaction schemes provided in Figure 1A. The success of the chain extension reaction from the PEG monomethyl ether (mPEG) substrate was confirmed by the presence of a single peak in the GPC analysis traces for the block copolymers, shifted to a higher molecular weight (lower elution volume) relatively to the mPEG substrate (Figure 1B).

The chemical composition of the copolymers was determined by ^{1}H NMR analysis, with typical spectra shown in Figure 1C for both copolymers. In the ^{1}H NMR spectra of both copolymers, peaks were present at 1.59, 5.24, 3.75 and 3.4 ppm. The peaks at 1.59 and 5.24 ppm are assigned to protons in -CH_3 groups and -CH- groups of the PLA chains, respectively, and the peaks at 3.75 and 3.4 ppm correspond to the protons in the PEG backbone and the methyl end group, respectively. As compared with the spectrum for PEG-*b*-PLA, the extra peaks at 4.7 and 1.2 ppm appearing in the spectrum for PEG-*a*-PLA are assigned to the -CH_3 and -CH- protons in the acetal group linking the PLA and PEG blocks.[41] The presence of the PLA and PEG components in the ^{1}H NMR spectrum further confirms the success of the procedures developed

for the synthesis of the PEG-*a*-PLA and PEG-*b*-PLA copolymers. The results of the GPC and NMR analyses for the block copolymers synthesized are summarized in Table 1.

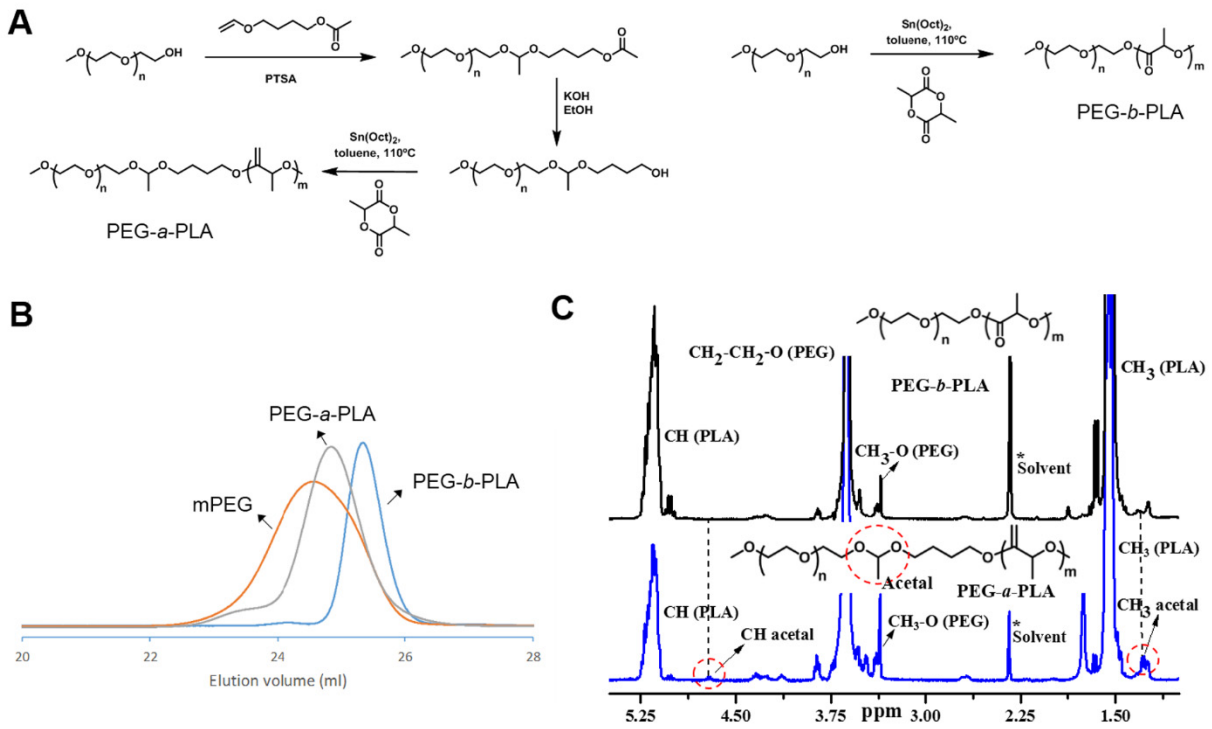

Figure 1. Synthesis and characterization of the copolymers: A. Synthetic routes for PEG-*a*-PLA and PEG-*b*-PLA; B. GPC traces for (from right to left) mPEG with M_n ~ 5000, PEG-*a*-PLA and PEG-*b*-PLA; C. ^{1}H NMR spectra for (top) PEG-*b*-PLA and (bottom) PEG-*a*-PLA.

Table 1. Results of GPC and NMR analysis for PEG-*a*-PLA and PEG-*b*-PLA. The mPEG block had M_n = 5000 and M_w/M_n = 1.04.

Copolymer	M_n	M_w/M_n	mol% PLA
PEG-*a*-PLA	11000	1.07	26

PEG-*b*-PLA	15000	1.16	45

3.2 Preparation and characterization of PEG-*a*-PLA micelles

The self-assembly of the PEG-*a*-PLA copolymer into micellar aggregates was induced by slow addition of a solvent selective for the PEG block (water) to a solution in a good solvent for both blocks (DMF). Under these conditions the hydrophobic PLA chain segments are expected to form the core, while the shell consists of hydrophilic PEG chain segments (Scheme 1).

The as-prepared PEG-*a*-PLA micelles, observed by TEM, had a spherical topology (Figure 2 A, B). It should be noted that Figure 2A shows the micelles prepared without heat treatment, while Figure 2B presents the micelles prepared with a one-cycle heat treatment. Interestingly, the micelles in Figure 2A show a non-uniform size ranging from tens of nanometer to hundreds of nanometer, while the latter shows micelles with a much more uniform size. This difference was also reflected in the DLS results given in Figure 2C: A unimodal peak with a hydrodynamic diameter around 100 nm and a polydispersity index of 0.12 was found in the intensity distribution plots for micelles prepared with one cycle of heat treatment, while two populations around 50 and 500 nm were observed for the micelles without treatment. A likely explanation for this is re-equilibration of the samples under closer to equilibrium conditions, as a result of gradual temperature changes. It should also be noted that additional heat treatment rounds did not yield significant differences in the size and size distribution of the micelles, which implies that the temperature variations led to more gradual variations in solvent quality in comparison to the slow addition of a non-solvent to the copolymer solution. The micelles prepared with a one-

cycle heat treatment were used for the subsequent studies throughout this paper, because nanoparticles in this size range (around 100 nm diameter) with a low polydispersity are believed to be optimal for prolonged circulation as well as balanced accumulation and penetration in tumors.[42]

In addition, the self-assembly of PEG-*a*-PLA copolymers into micellar aggregates was verified by ^{1}H NMR analysis through the measurement of diffusion constants (Figure S1 and Table S1). Moreover, the CMC of PEG-*a*-PLA was measured to be 6.3×10^{-3} mg/mL by fluorescence spectroscopy (Figure S2). Detailed results and discussion of these topics can be found in the Supporting Information.

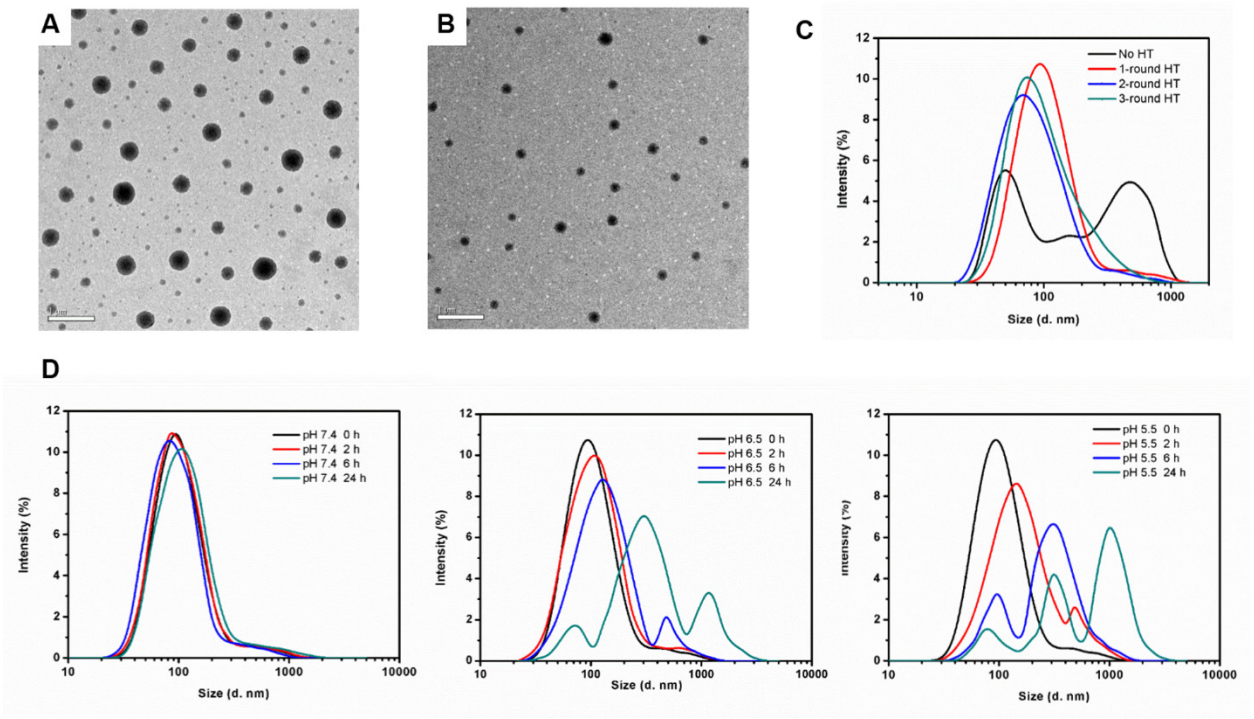

Figure 2. Topology and size of the micelles: A. TEM image for PEG-*a*-PLA micelles without heat treatment. Scale bar: 1 μm; B. TEM image for PEG-*a*-PLA micelles after one cycle of heat treatment. Scale bar: 1 μm; C. Size distribution from DLS of PEG-*a*-PLA micelles with and

without heat treatment. The size is expressed as the hydrodynamic diameter (d, nm). HT: heat treatment; D. Change in hydrodynamic diameter (d, nm) of PEG-*a*-PLA micelles in PBS solutions at different pH by DLS.

3.3 pH-induced size changes of PEG-*a*-PLA micelles

The pH responsiveness of the PEG-*a*-PLA micelles was investigated by monitoring size changes in PBS at different pH (i.e. 7.4, 6.5 and 5.5) as a function of time using DLS. It can be seen in Figure 2D that the particle size maintained almost unchanged (around 100 nm) after treatment in PBS at pH 7.4 for up to 24 h, confirming that the micelles were stable in this environment. When the pH was decreased to 6.5, it was found that the size of the micelles was essentially unchanged after 2 h of treatment, but tended to increase with a broader distribution after 6 h, which shows that the micelles became unstable, presumably due to partial PEG chain shedding and aggregate formation by the PLA cores. The instability of the micelles became more obvious, with the formation of more and larger aggregates, after 24 h of treatment in PBS at pH 6.5. It can also be seen in Figure 2D that the size of the particles increased more rapidly in PBS at pH 5.5 as compared to pH 6.5. This implies that the micelles were destabilized and formed aggregates more rapidly as a result of the accelerated hydrolysis of acetal bonds at the lower pH. It has been similarly reported that fast aggregation could be induced in the presence of glutathione or dithiothreitol for redox-sensitive shell-sheddable micelles such as poly(ethylene glycol)-SS-poly(ε-caprolactone) (PEG-SS-PCL)[21] and poly(ethylene glycol)-SS-poly(2,4,6-trimethoxybenzylidene-pentaerythritol carbonate) (PEG-SS-PTMBPEC).[22] The stability of the micelles in cell culture medium at 37°C with 10% FBS was also studied. No significant changes in size were observed for the micelles after incubation for 24 h (Figure S3). The results obtained therefore suggest that the PEG-*a*-PLA micelles should be stable in human blood, while the PEG

shell would become sheddable in response to the mildly acidic tumoral environment, especially in the intracellular endosome.

3.4 Drug loading and simulated release *in vitro*

A calibration curve relating the paclitaxel concentration X (μg/mL) in acetonitrile to the response was obtained as $Y = 0.00299\ X - 8.73 \times 10^{-4}$ ($R^2 = 0.998$, where Y presents the HPLC peak area, in arbitrary units). Using Equations (1) and (2) provided in Section 2.4 in combination with the calibration curve, the entrapment efficiency (EE%) and drug loading capacity (DLC%) of the PEG-*a*-PLA micelles were calculated to be 68.7% and 6.9 wt%, respectively.

The *in vitro* PTX release profiles from M-PTX at different pH are compared in Figure 3. It can be seen that both M-PTX and M*b*-PTX displayed sustained PTX release behavior over a period of 72 h, with cumulative release of 45% and 38%, respectively, after 72 h at pH 7.4. The slightly lower release for M*b*-PTX over M-PTX at pH 7.4 may be due to the larger size of M*b*-PTX micelles (around 200 nm). The influence of particle size on the drug release rate was investigated previously.[43] However, much faster and more effective PTX release was observed for M-PTX at pH 6.5 as compared to M*b*-PTX. The cumulative release of PTX from M-PTX reached 48% after 24 h at pH 6.5 and increased to 70% after 72 h, while M*b*-PTX did not show as much change at pH 6.5 as compared with pH 7.4, with cumulative PTX release of 25% and 39% after 24 and 72 h, respectively. Moreover, at pH 5.5 the PTX release from M-PTX was further accelerated as compared to pH 6.5. The cumulative release of PTX under these conditions reached 70% and 90 % after 24 and 72 h, respectively. As a control, the free PTX solution showed a burst release of PTX with cumulative release over 90% after 12 h, irrespective of the pH. The increased drug release rate and improved cumulative release from M-PTX at pH 6.5 and 5.5 are attributed to the

acid-triggered PEG chain shedding from the micelles. Furthermore, drug release was increased at the lower pH as a result of accelerated PEG chain shedding. These pH-triggered drug release profiles for M-PTX suggest that the PEG-*a*-PLA micelles could serve as efficient vehicles for tumor-targeted drug delivery.

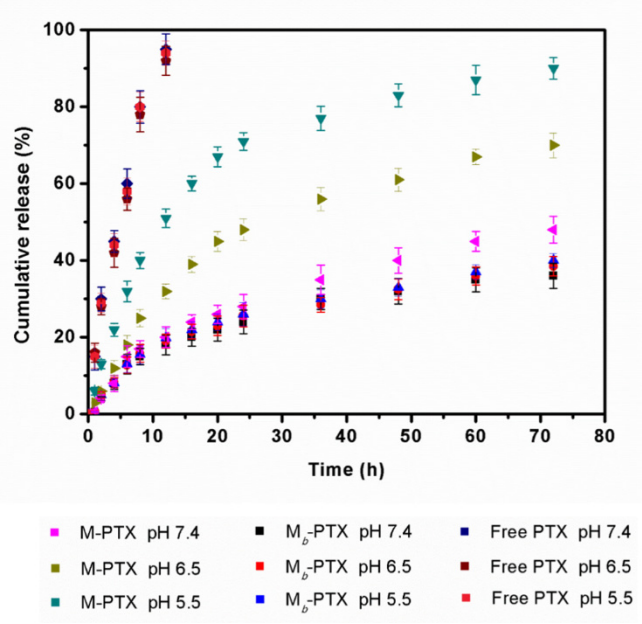

Figure 3. Release profiles for PTX from M-PTX, M*b*-PTX and free PTX in PBS solutions at different pH in the presence of 1 M sodium salicylate at 37 ℃.

3.5 Cellular toxicity of blank micelles

The cytotoxicity of blank PEG-*a*-PLA micelles was evaluated with different cell lines including Hela cells, L-02 cells and HUVEC. Cell viability, calculated using Equation (3) given in Section 2.5, is provided in Figure 4. It is clear that the micelles were not toxic to Hela cells (Figure 4A), as cell viability was higher than 100% after incubation for 72 h at a micellar concentration of 200 μg/mL. No obvious changes in Hela cell viability were observed for different micellar concentrations (from 2 to 200 μg/mL) and incubation periods (24, 48, 72 h). The cytotoxicity of

blank PEG-*a*-PLA micelles to L-02 cells and HUVEC is depicted in Figure 4B and Figure 4C, respectively. Again, the micelles showed no obvious cytotoxicity to L-02 cells and HUVEC for different concentrations (from 2 to 200 μg/mL) and incubation times (24, 48, 72 h for L-02 cells; 24, 72, 120 h for HUVEC) with a cell viability of over 90%. These results indicate that the PEG-*a*-PLA micelles are highly biocompatible and could be useful for biomedical applications.

3.6 Cellular internalization of fluorescently labeled micelles

The cellular internalization of the PEG-*a*-PLA micelles was studied using C6-labeled micelles (M-C6). It can be seen from Figure 4D that the fluorescent dye encapsulated in M-C6 and the C6-labeled non-responsive micelles (M_b-C6) entered the cytoplasm of Hela cells more efficiently than free C6. This suggests that encapsulated C6 entered the cells through a carrier-mediated endocytosis pathway, while free C6 was internalized more gradually by diffusion. This is consistent with previous studies in which the authors claimed that encapsulated drugs entered the cells through carrier-mediated endocytosis, followed by intracellular release.[44, 45] It is interesting to note that the cellular internalization efficiency of M-C6 subjected to treatment with PBS at pH 6.5 for 2 and 6 h was enhanced slightly as compared with M-C6 without treatment, while it decreased markedly for M-C6 incubated at pH 6.5 for 24 h. This can be explained as follows: The micelles were slowly destabilized at pH 6.5, with a relatively low extent of PEG chain shedding after 2 and 6 h, that was insufficient to form large aggregates but facilitated the cellular uptake of the particles to some extent. It has been indeed suggested that PEG chain shedding can facilitate the cellular internalization of nanoparticles.[13-15] Wang et al.[13] thus reported tumor-pH responsive polymeric nanoparticles based on block copolymers of PEG and poly(D,L-lactic acid). They concluded that both the release of the PEG corona and an increase in zeta potential of the nanoparticles could facilitate cellular uptake. In the current case, the C6 molecules were

presumably also delivered into the cells mainly through carrier-mediated endocytosis. In contrast, the extent of PEG chain shedding was much increased after 24 h of treatment and large aggregates formed, which is expected to impede cellular uptake.[43] In that case the C6 molecules first diffused out of the aggregates and entered the cells similarly to the free dye. It is known that the retention time of nanoparticles in the extracellular environment before cellular uptake is normally rather short (less than 6 h).[46, 47] Therefore, it is believed on the basis of these results that the PEG-*a*-PLA micelles loaded with drug should be internalized by tumor cells *in vivo* efficiently.

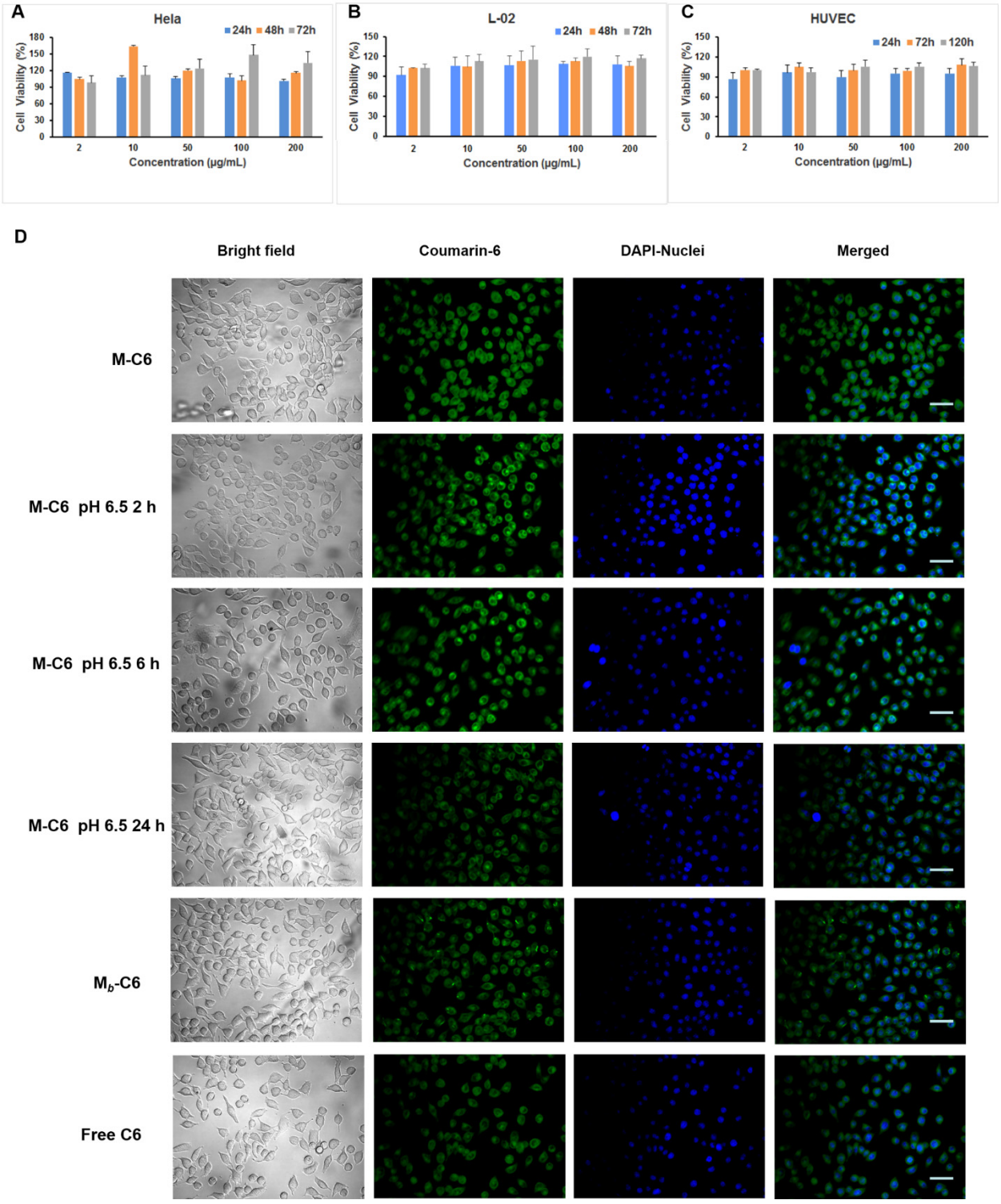

Figure 4. Cytotoxicity of blank PEG-*a*-PLA micelles determined by CCK-8 analysis with different cell lines: A. Hela cells; B. L-02 cells; C. HUVEC; D. Cellular internalization of PEG-*a*-PLA micelles fluorescently labeled with C6. M-C6 represents C6-labeled PEG-*a*-PLA micelles

without treatment; M*b*-C6 represents C6-labeled non-responsive PEG-*b*-PLA micelles; "M-C6 pH 6.5 *x* h" denote the C6-labeled PEG-*a*-PLA micelles subjected to treatment with PBS at pH 6.5 for *x* h. Scale bar: 50 μm.

3.7 Anti-tumor efficacy *in vitro*

Cellular proliferation assay

The *in vitro* cytotoxicity of M-PTX to Hela cells was evaluated by the CCK-8 assay. To simulate the extracellular tumor space, the pH of the culture medium for Hela cells was adjusted to 6.5 with 0.1 M HCl before treatment with various PTX formulations. It was first verified that pH 6.5 did not affect cell viability, in that cell viability was as high as in normal culture medium (Figure 5A). Similar treatment and results were reported in the literature, where the authors demonstrated that even pH 5.8 did not affect tumor cell viability.[48] It can been seen in Figure 5A that the cytotoxicity of all the PTX formulations increased with the PTX concentration. It is worth noting that the cytotoxicity of M-PTX at pH 6.5 was significantly enhanced as compared to M*b*-PTX and free PTX when the PTX concentration was over 0.1 μg/mL, while the cytotoxicity of M-PTX under normal conditions was only slightly higher than for M*b*-PTX and free PTX when the PTX concentration was 0.4 μg/mL. The enhanced cytotoxicity of M-PTX at pH 6.5 over M*b*-PTX and free PTX could be due to the increased cellular internalization and pH-triggered rapid intracellular drug release.

To further study the effects of M-PTX on cellular proliferation, the cell cycle progression of Hela cells treated with the different PTX formulations for 48 h was analyzed by flow cytometry. According to Figure 5B, in comparison with the control, the PTX formulations (M-PTX, M*b*-PTX and free PTX) in normal culture medium led to a remarkable increase in the accumulation

of G2 phase cells, which increased from 13.2% (control) to 40.5% (M-PTX), 22.3% (M_b-PTX) and 29.4% (free PTX), indicating that these PTX formulations affected cellular proliferation by the same mechanism. It is well-known that PTX can induce cell cycle arrest in the G2 phase of mitosis, resulting in the restraint of cell proliferation.[49, 50] The superior proliferation inhibition for M-PTX is ascribed to increased cellular internalization (over free PTX) and fast intracellular drug release (as compared to M_b-PTX). Moreover, it should be noted that M-PTX at pH 6.5 yielded further increase in accumulation of G2 phase cells as compared to the normal culture medium. This could be explained by enhanced internalization of the pH-sensitive micelles at pH 6.5 over the normal culture medium, as described in Section 3.6.

Cellular apoptosis assay

The induction of Hela cell apoptosis by the various PTX formulations was quantified by flow cytometry. It was found that M-PTX at pH 6.5 gave the highest percentage of cellular apoptosis (including early and late apoptosis) as compared to the other formulations (Figure S4). In addition, the gene expression assays indicated that M-PTX induced cellular apoptosis in the same manner as free PTX, which is by promoting the expression of *caspase-3* while inhibiting the expression of Caspase, *PCNA*, B-cell leukemia/lymphoma-2 (*BCL-2)* (Figure S5). The enhanced cellular apoptosis caused by M-PTX at pH 6.5 can be likewise attributed to the synergistic effect of enhanced cellular internalization and pH-triggered intracellular drug release.

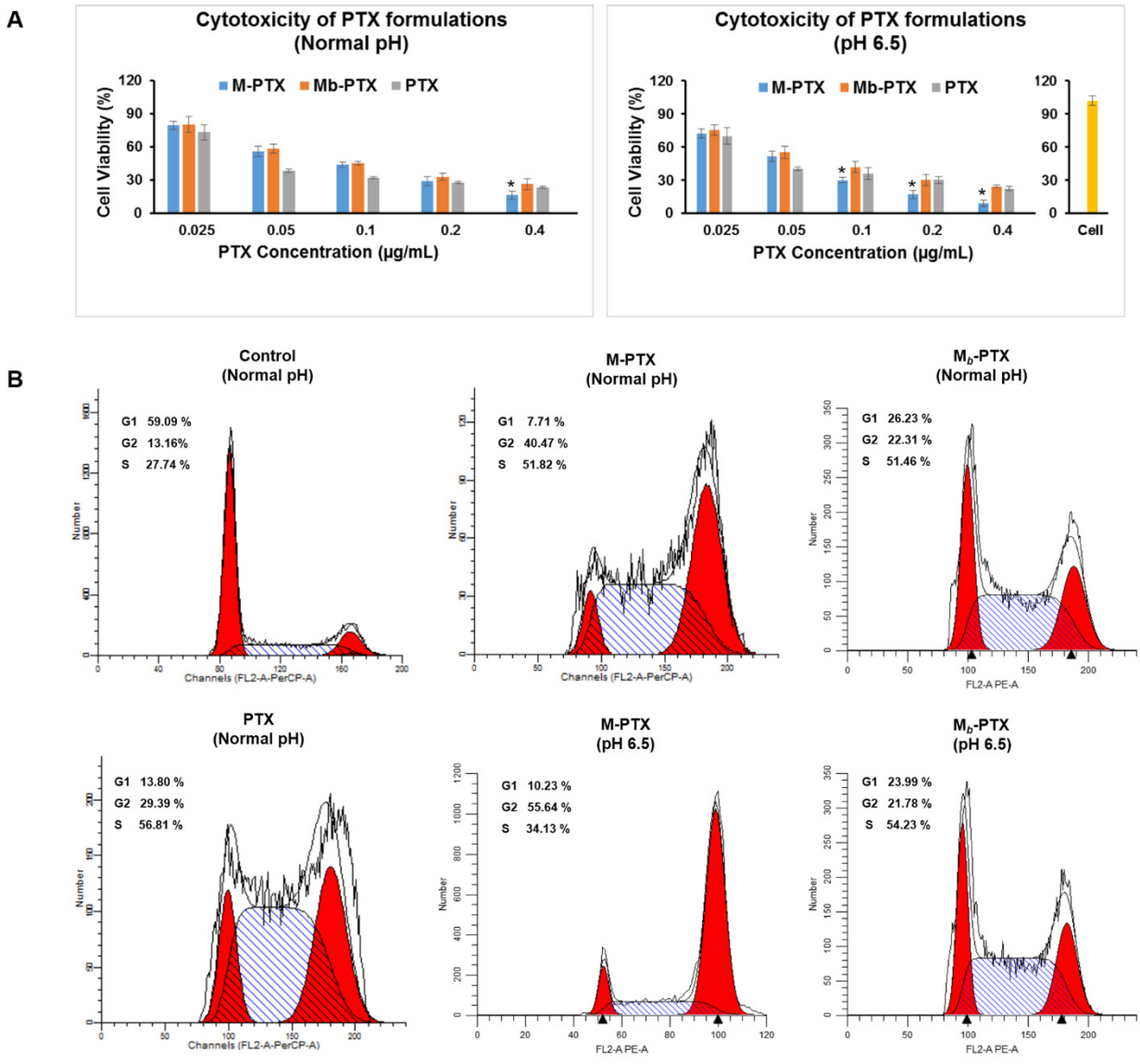

Figure 5. *In vitro* antitumor activity of M-PTX for Hela cells. A. Cytotoxicity of the different PTX formulations determined by CCK-8 analysis. Significant differences compared with M*b*-PTX **P* < 0.05. B. Cell cycle distributions of cells treated with the different PTX formulations for 48 h.

3.8 Anti-tumor efficacy *in vivo*

Tumor targeting efficacy

The *in vitro* drug release and cellular internalization studies demonstrated that the micelles could be useful as carriers for drug delivery with pH responsiveness. To further evaluate the potential of the micelles as anti-tumor drug carriers, *in vivo* tumor targeting efficacy was investigated with a living fluorescence imaging system. The mice were injected through the tail vein with M-C6, or with C6 as a control. As shown in Figure 6A, the control group yielded a decreasing fluorescence intensity in the tumor area with the post-injection time. The fluorescence intensity in the tumor area was rather low at 6 h post-injection and decreased rapidly over the next 18 h, because of the animal metabolism. After 48 h post-injection, the fluorescence in the tumor area almost completely disappeared for the control group. In contrast, the fluorescence intensity in the tumor area was much higher for the mice injected with M-C6 than for the control group. It was also found that fluorescence accumulation in the tumor area increased with time within 24 h post-injection. The fluorescence intensity in the tumor area for both groups is quantified in Figure 6B. It can be seen that the radiation efficiency of fluorescence in the tumor area for the M-C6 group was approximately six times as high as for the control group at 24 h post-injection. The differences in C6 accumulation in the tumor area between the M-C6 and control groups was also reflected in the fluorescence images of tumor sections at 24 and 48 h post-injection, shown in Figure 6C. It is apparent that C6 accumulation in tumor tissues was much higher in the M-C6 group than in the control group after 24 h, while the difference between the two groups became smaller after 48 h because of the animal metabolism, which is in agreement with the results of Figures 6A and 6B. The above results indicate that the micelles could significantly prolong the circulation time of C6 *in vivo* with the protective effect of PEG, and promote accumulation in the tumor area through a passive targeting mechanism, that is mainly the enhanced permeability and retention (EPR) effect. However it should be clarified that M-C6 is not expected to show tumor-

specific targeting ability beyond the EPR effect, since no targeting ligands were employed in the present micellar system.

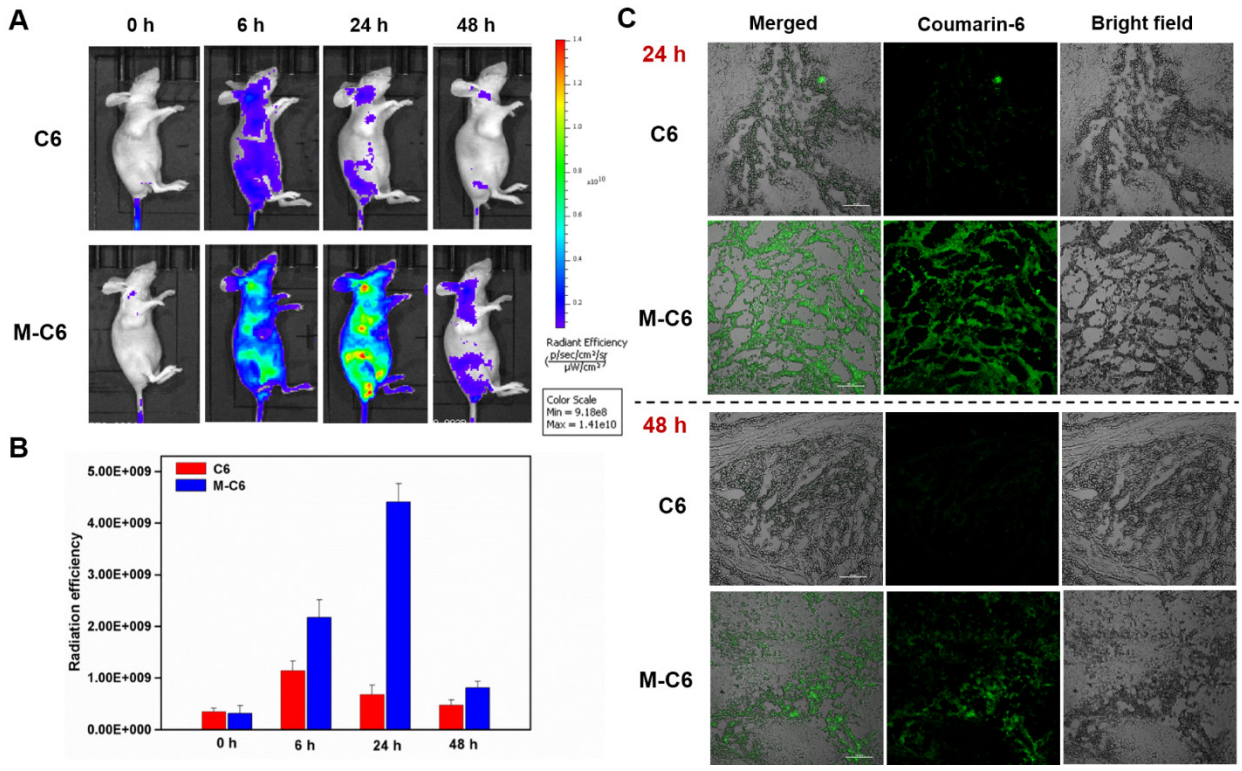

Figure 6. Tumor-targeting efficacy of M-C6. A. *In vivo* time-dependent fluorescence images 0, 6, 24 and 48 h after the administration of M-C6 and free C6. The color bar (from red to blue) indicates changes in fluorescence radiation efficiency from high to low. B. Quantification of the tumor-targeting characteristics of M-C6 and free C6. C. Fluorescence images for tumor sections at 24 and 48 h post-injection of M-C6 and free C6. Scale bar: 100 μm.

Antitumor efficacy

Due to the prolonged circulation time and enhanced tumor localization, M-PTX was expected to have good antitumor efficacy *in vivo*. Hela tumor-bearing mice were used to evaluate the *in vivo* antitumor potential of M-PTX. The measurements of tumor volume and body weight of the mice

treated with successive tail vein injections of different PTX formulations are shown in Figure 7A. It can be seen that from the fifth dose to the last, the M-PTX and PTX groups displayed smaller tumor volumes as compared to the control group, while the M-PTX group showed the smallest tumor volumes. Moreover, the differences between these groups became more significant as the treatment time increased. These results reveal that the pH-responsive micelles enhance the antitumor efficacy of PTX. In addition, the body weight of mice showed no significant differences among the groups throughout the treatment. Pictures of the final tumors harvested from the mice after the treatments, and images of HE-stained tumor sections are presented in Figure 7B. Tumor cells with a spherical or spindle shape were observed in the control group, suggesting good growth of the tumor. On the contrary, cellular necrosis and dead cells with condensed nuclei could be seen in the PTX and M-PTX groups. Moreover, the largest number of dead cells with condensed nuclei was observed in the M-PTX group, which provides substantial evidence for enhanced antitumor efficacy of PTX combined with the micelles.[51] To further investigate the *in vivo* antitumor efficacy of M-PTX, an immunohistochemical study including TUNEL assay and PCNA expression was also performed with the tumor sections (Figure 7C). In agreement with the results for the tumor growth rate and the HE-stained tissue observations, the M-PTX group presented the largest number of TUNEL-positive tumor cells and the lowest expression of PCNA, which means that the M-PTX treatment was most efficient at inhibiting the proliferation and inducing death in tumor cells.[52]

There have been many reports on shell-sheddable micellar systems for tumor-targeted drug delivery in recent years, among which a few carefully designed systems exhibited superior antitumor efficacy *in vivo*. A good example of this is cRGD-functionalized reduction-responsive shell-sheddable disulfide-linked PEG-SS-PCL block copolymers for the intracellular delivery of

doxorubicin developed by Zhong and coworkers.[53] This system displayed efficient tumoral accumulation and fast drug release in tumor cells, with superior therapeutic outcomes for human glioma xenografts *in vivo*. Additionally, with the non-cRGD-functionalized PEG-SS-PCL micellar system, remarkable antitumor efficacy *in vivo* could be accomplished by injecting exogenous vitamin C when tumor accumulation of the drug-loaded micelles reached their highest level. This is because vitamin C acted as a reducing agent, which triggered the rapid extracellular drug release from the micelles.[54] In the current investigation, a simple pH-sensitive PLA-*a*-PEG micellar system with a sheddable shell was designed for tumor-targeted drug delivery. The shell-shedding and drug release behaviors of M-PTX in simulated tumoral extracellular and intracellular environments were compared systematically. The *in vivo* performance demonstrated that M-PTX could efficiently inhibit tumor growth. The possible reasons for the enhanced antitumor efficacy of M-PTX over free PTX could be explained as follows: Firstly, the PEG shell should stabilize the particles and prolong their circulation time in the bloodstream, leading to enhanced tumoral accumulation by passive targeting *via* the EPR effect. Secondly, after the particles arrive at the tumor sites, partial PEG shedding is induced by the mildly acidic extracellular space (pH 6.5-7.2), which can promote cellular internalization of the particles to some extent (with a small amount of drug released in the extracellular space). Finally, the shell of the particles degrades extensively, with efficient drug release triggered by the lower pH (5.0-6.0) in the endosome, thus achieving a high antitumor efficacy. However, it is admittedly a limitation of this work that the relevance of pH-sensitive shell-shedding *in vivo* was not fully demonstrated, since no results were obtained for the corresponding insensitive micelles (M_b-PTX).

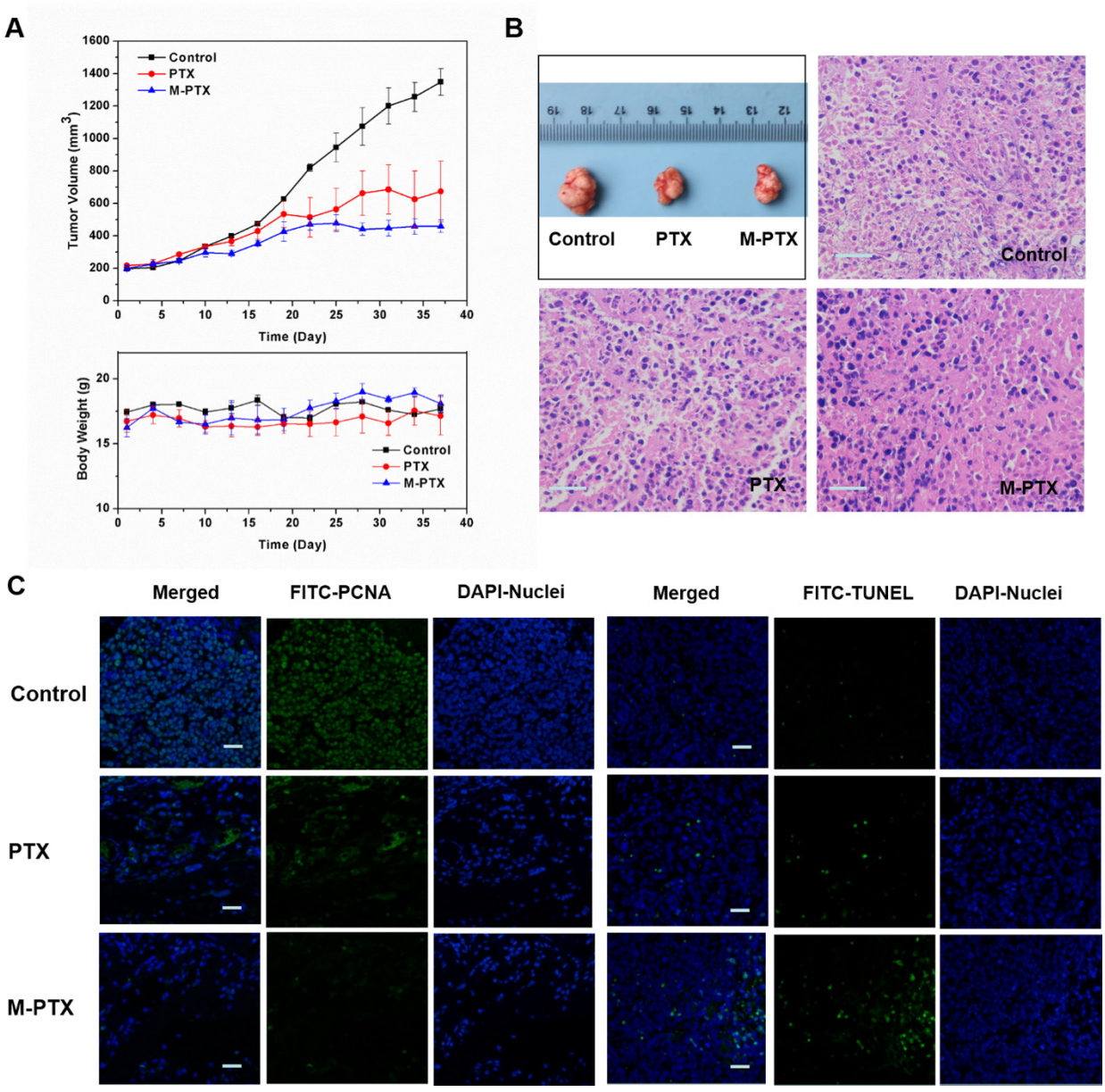

Figure 7. *In vivo* antitumor efficacy of M-PTX. A. Changes in the tumor volume and body weight of the Hela tumor-bearing nude mice receiving intravenous injections of M-PTX and free PTX. B. Representative images for HE-stained tumor sections after treatment with M-PTX and free PTX. Scale bar: 100 μm. C. PCNA and TUNEL assays of tumor sections after treatment with M-PTX and free PTX. Scale bar: 100 μm.

4. CONCLUSIONS

A PEG-*a*-PLA micellar system with pH responsiveness was developed, characterized and evaluated *in vitro* and *in vivo* as carrier for tumor-targeted drug delivery. The spherical micelles, with an average diameter of ca. 100 nm, were stable in PBS at pH 7.4, but responded to mildly acidic conditions with more rapid drug release. It was found that the drug-loaded micelles efficiently inhibited cellular proliferation and promoted the apoptosis of Hela cells *in vitro*, and inhibited tumor growth *in vivo* without obvious harmful side effects. The enhanced antitumor efficacy of PTX-loaded micelles over free PTX is attributed to a synergistic effect of several factors including a significantly prolonged circulation time, enhanced cellular internalization, and pH-triggered intracellular drug release. Since both PEG and PLA are FDA-approved for biological use due to their excellent biocompatibility and biodegradability, the pH-responsive PEG-*a*-PLA micellar system has great prospects in clinical applications as drug carriers for cancer treatment.

ASSOCIATED CONTENT

Supporting Information. The Supporting Information is available free of charge on the ACS Publications website at DOI:***

Information on the source, culture and incubation conditions of cell lines, synthetic procedures and characterization methods for the copolymers, ^{1}H NMR spectra for PEG-*a*-PLA before and after self-assembly, measurement of diffusion coefficients for the copolymer chain segments before and after self-assembly, measurement of the CMC of the copolymers, the results of stability of micelles of PEG-*a*-PLA in cell culture medium at 37°C in the presence of 10% FBS, the results of cellular apoptosis assay of Hela cells with various PTX formulations using flow

cytometry, the results and some discussion of gene expression after 48 h for cells treated with M-PTX and free PTX. (PDF)

AUTHOR INFORMATION

Corresponding Authors

* E-mail: yang_sunny@yahoo.com. Tel: +86 27-87793523. Fax: +86 27-87792265.

* E-mail: gauthier@uwaterloo.ca. Tel: +1-519- 888-4567 ext. 35205. Fax: +1-519-746-0435

Author Contributions

The manuscript was written through contributions of all the authors. All authors have given approval to the final version of the manuscript.

‡ Lin Xiao and Lixia Huang contributed equally to this work.

Funding Sources

China Postdoctoral Science Foundation (General Program, No. 2015M580640) and National Natural Science Foundation of China (General Program, No. 21574050).

Notes

The authors declare no competing financial interest.

ACKNOWLEDGMENT

The authors acknowledge the China Postdoctoral Science Foundation (General Program, No. 2015M580640) and the National Natural Science Foundation of China (General Program, No. 21574050) for their financial support. The support of the Natural Sciences and Engineering Research Council of Canada (NSERC) is also gratefully acknowledged. The authors would like

to thank the Analytical and Testing Center of the Huazhong University of Science and Technology for part of the instruments used in this work. The authors are also grateful to Prof. Ping Zhou and Prof. Xianqin Zhang at Huazhong University of Science and Technology, and Prof. Zhihong Wu at Peking Union Medical College Hospital for their generous gifts of cell lines.

ABBREVIATIONS

PEG-*a*-PLA, acetal-linked poly(ethylene glycol)-*block*-polylactide; PEG-*b*-PLA, poly(ethylene glycol)-*block*-polylactide; PTX, paclitaxel; C6, coumarin-6; M-PTX, PTX-loaded PEG-*a*-PLA micelles; M$_b$-PTX, PTX-loaded PEG-*b*-PLA micelles; M-C6, coumarin-6 labeled PEG-*a*-PLA micelles; M$_b$-C6, coumarin-6 labeled PEG-*b*-PLA micelles.

REFERENCES

(1) Jeong, J. H.; Kim, S. W.; Park, T. G. Molecular Design of Functional Polymers for Gene Therapy. *Prog. Polym. Sci.* **2007**, *32*, 1239-1274.

(2) Obst, M.; Steinbüchel, A. Microbial Degradation of Poly (amino acid)s. *Biomacromolecules* **2004**, *5*, 1166-1176.

(3) Lee, J. S.; Go, D. H.; Bae, J. W.; Lee, S. J.; Park, K. D. Heparin Conjugated Polymeric Micelle for Long-Term Delivery of Basic Fibroblast Growth Factor. *J. Controlled Release* **2007**, *117*, 204-209.

(4) Li, C.; Wallace, S. Polymer-Drug Conjugates: Recent Development in Clinical Oncology. *Adv. Drug Delivery Rev.* **2008**, *60*, 886-898.

(5) Knop, K.; Hoogenboom, R.; Fischer, D.; Schubert, U. S. Poly(ethylene glycol) in Drug Delivery: Pros and Cons as Well as Potential Alternatives. *Angew. Chem., Int. Ed.* **2010**, *49*, 6288-6308.

(6) Raeesi, V.; Chou, L. Y.; Chan, W. C. Tuning the Drug Loading and Release of DNA‐Assembled Gold‐Nanorod Superstructures. *Adv. Mater.* **2016**, *28*, 8511-8518.

(7) Xu, X.; Wu, J.; Liu, Y.; Yu, M.; Zhao, L.; Zhu, X.; Bhasin, S; Li, Q.; Ha, E.; Shi, J.; Farokhzad, O. C. Ultra‐pH‐Responsive and Tumor‐Penetrating Nanoplatform for Targeted siRNA Delivery with Robust Anti‐Cancer Efficacy. *Angew. Chem., Int. Ed.* **2016**, *55*, 7091-7094.

(8) Kim, J.; Lee, Y. M.; Kim, H.; Park, D.; Kim, J.; Kim, W. J. Phenylboronic Acid-Sugar Grafted Polymer Architecture as a Dual Stimuli-Responsive Gene Carrier for Targeted Anti-Angiogenic Tumor Therapy. *Biomaterials* **2016**, *75*, 102-111.

(9) Cho, H. J.; Yoon, I. S.; Yoon, H. Y.; Koo, H.; Jin, Y. J.; Ko, S. H.; Shim, J. S.; Kim, K.; Kwon, I. C.; Kim, D. D. Polyethylene Glycol-Conjugated Hyaluronic Acid-Ceramide Self-Assembled Nanoparticles for Targeted Delivery of Doxorubicin. *Biomaterials* **2012**, *33*, 1190-1200.

(10) Zhang, Y.; Wang, X. J.; Guo, M.; Yan, H. S.; Wang, C. H.; Liu, K. L. Cisplatin-Loaded Polymer/Magnetite Composite Nanoparticles as Multifunctional Therapeutic Nanomedicine. *Chin. J. Polym. Sci.* **2014**, *32*, 1329-1337.

(11) Mishra, S.; Webster, P.; Davis, M. E. PEGylation Significantly Affects Cellular Uptake and Intracellular Trafficking of Non-Viral Gene Delivery Particles. *Eur. J. Cell Biol.* **2004**, *83*, 97-111.

(12) Gratton, S. E.; Ropp, P. A.; Pohlhaus, P. D.; Luft, J. C.; Madden, V. J.; Napier, M. E.; DeSimone, J. M. The Effect of Particle Design on Cellular Internalization Pathways. *Proc. Natl. Acad. Sci.* **2008**, *105*, 11613-11618.

(13) Sun, C. Y.; Liu, Y.; Du, J. Z.; Cao, Z. T.; Xu, C. F.; Wang, J. Facile Generation of Tumor‐pH‐Labile Linkage‐Bridged Block Copolymers for Chemotherapeutic Delivery. *Angew. Chem. Int. Edit.* **2016**, *55*, 1010-1014.

(14) Yang, X. Z.; Du, J. Z.; Dou, S.; Mao, C. Q.; Long, H. Y.; Wang, J. Sheddable Ternary Nanoparticles for Tumor Acidity-Targeted siRNA Delivery. *ACS Nano* **2012**, *6*, 771-781.

(15) Poon, Z.; Chang, D.; Zhao, X.; Hammond, P. T. Layer-by-Layer Nanoparticles with a pH-Sheddable Layer for in Vivo Targeting of Tumor Hypoxia. *ACS Nano* **2011**, *5*, 4284-4292.

(16) Wei, H.; Zhuo, R. X.; Zhang, X. Z. Design and Development of Polymeric Micelles with Cleavable Links for Intracellular Drug Delivery. *Prog. Polym. Sci.* **2013**, *38*, 503-535.

(17) Li, S. D.; Huang, L. Stealth Nanoparticles: High Density but Sheddable PEG is a Key for Tumor Targeting. *J. Controlled Release* **2010**, *145*, 178-181.

(18) Chen, J.; Qiu, X.; Ouyang, J.; Kong, J.; Zhong, W.; Xing, M. M. pH and Reduction Dual-Sensitive Copolymeric Micelles for Intracellular Doxorubicin Delivery. *Biomacromolecules* **2011**, *12*, 3601-3611.

(19) Zhong, Y.; Yang, W.; Sun, H.; Cheng, R.; Meng, F.; Deng, C.; Zhong, Z. Ligand-Directed Reduction-Sensitive Shell-Sheddable Biodegradable Micelles Actively Deliver Doxorubicin into the Nuclei of Target Cancer Cells. *Biomacromolecules* **2013**, *14*, 3723-3730.

(20) Sun, H.; Guo, B.; Li, X.; Cheng, R.; Meng, F.; Liu, H.; Zhong, Z. Shell-Sheddable Micelles Based on Dextran-SS-poly (ε-caprolactone) Diblock Copolymer for Efficient Intracellular Release of Doxorubicin. *Biomacromolecules* **2010**, *11*, 848-854.

(21) Sun, H.; Guo, B.; Cheng, R.; Meng, F.; Liu, H.; Zhong, Z. Biodegradable Micelles with Sheddable Poly (ethylene glycol) Shells for Triggered Intracellular Release of Doxorubicin. *Biomaterials* **2009**, *30*, 6358-6366.

(22) Chen, W.; Zhong, P.; Meng, F.; Cheng, R.; Deng, C.; Feijen, J.; Zhong, Z. Redox and pH-Responsive Degradable Micelles for Dually Activated Intracellular Anticancer Drug Release. *J. Controlled Release* **2013**, *169*, 171-179.

(23) Guan, X.; Guo, Z.; Wang, T.; Lin, L.; Chen, J.; Tian, H.; Chen, X. A pH-Responsive Detachable PEG Shielding Strategy for Gene Delivery System in Cancer Therapy. *Biomacromolecules* **2017**, *18*, 1342-1349.

(24) Zhao, C.; Shao, L.; Lu, J.; Deng, X.; Wu, Y. Tumor Acidity-Induced Sheddable Polyethylenimine-Poly (trimethylene carbonate)/DNA/Polyethylene Glycol-2, 3-Dimethylmaleicanhydride Ternary Complex for Efficient and Safe Gene Delivery. *ACS Appl. Mater. Interfaces* **2016**, *8*, 6400-6410.

(25) Car, A.; Baumann, P.; Duskey, J. T.; Chami, M.; Bruns, N.; Meier, W. pH-Responsive PDMS-b-PDMAEMA Micelles for Intracellular Anticancer Drug Delivery. *Biomacromolecules* **2014**, *15*, 3235-3245.

(26) Kanamala, M.; Wilson, W. R.; Yang, M.; Palmer, B. D.; Wu, Z. Mechanisms and Biomaterials in pH-Responsive Tumour Targeted Drug Delivery: A Review. *Biomaterials* **2016**, *85*, 152-167.

(27) Liu, Y.; Wang, W.; Yang, J.; Zhou, C.; Sun, J. pH-Sensitive Polymeric Micelles Triggered Drug Release for Extracellular and Intracellular Drug Targeting Delivery. *Asian J Pharm Sci* **2013**, *8*, 159-167.

(28) Chen, W.; Meng, F.; Cheng, R.; Zhong, Z. pH-Sensitive Degradable Polymersomes for Triggered Release of Anticancer Drugs: a Comparative Study with Micelles. *J. Controlled Release* **2010**, *142*, 40-46.

(29) Oishi, M.; Nagasaki, Y.; Itaka, K.; Nishiyama, N.; Kataoka, K. Lactosylated Poly (ethylene glycol)-siRNA Conjugate Through Acid-Labile β-Thiopropionate Linkage to Construct pH-Sensitive Polyion Complex Micelles Achieving Enhanced Gene Silencing in Hepatoma Cells. *J. Am. Chem. Soc.* **2005**, *127*, 1624-1625.

(30) Liu, N.; Tan, Y.; Hu, Y.; Meng, T.; Wen, L.; Liu, J.; Cheng, B.; Yuan, H.; Huang, X.; Hu, F. A54 Peptide Modified and Redox-Responsive Glucolipid Conjugate Micelles for Intracellular Delivery of Doxorubicin in Hepatocarcinoma Therapy. *ACS Appl. Mater. Interfaces* **2016**, *8*, 33148-33156.

(31) Stephen, Z. R.; Kievit, F. M.; Veiseh, O.; Chiarelli, P. A.; Fang, C.; Wang, K.; Hatzinger, S. J.; Ellenbogen, R. G.; Silber, J. R.; Zhang, M. Redox-Responsive Magnetic Nanoparticle for Targeted Convection-Enhanced Delivery of O6-Benzylguanine to Brain Tumors. *ACS Nano* **2014**, *8*,10383-10395.

(32) Nazli, C.; Demire, G. S.; Yar, Y.; Acar, H. Y.; Kizilel, S. Targeted Delivery of Doxorubicin into Tumor Cells *via* MMP-Sensitive PEG Hydrogel-Coated Magnetic Iron Oxide Nanoparticles (MIONPs). *Colloids Surf., B.* **2014**, *122*, 674-683.

(33) Ramot, Y.; Haim-Zada M.; Domb, A. J.; Nyska, A. Biocompatibility and Safety of PLA and Its Copolymers. *Adv. Drug Delivery Rev.* **2016**, *107*, 153-162.

(34) Tyler, B.; Gullotti, D.; Mangraviti, A.; Utsuki, T.; Brem, H. Polylactic acid (PLA) Controlled Delivery Carriers for Biomedical Applications. *Adv. Drug Delivery Rev.* **2016**, *107*, 163-175.

(35) Lale, S. V.; Kumar, A.; Prasad, S.; Bharti, A. C.; Koul, V. Folic Acid and Trastuzumab Functionalized Redox Responsive Polymersomes for Intracellular Doxorubicin Delivery in Breast Cancer. *Biomacromolecules* **2015**, *16*, 1736-1752.

(36) Xiao, R. Z.; Zeng, Z. W.; Zhou, G. L.; Wang, J. J.; Li, F. Z.; Wang, A. M. Recent Advances in PEG-PLA Block Copolymer Nanoparticles. *Int. J. Nanomed.* **2010**, *5*, 1057-1065.

(37) Hashimoto, T.; Mori, H.; Urushisaki, M. Poly (tetramethylene ether) Glycol Containing Acetal Linkages: New PTMG‐Based Polyol for Chemically Recyclable Polyurethane Thermoplastic Elastomer. *J. Polym. Sci., Part A: Polym. Chem.* **2008**, *46*, 1893-1901.

(38) Chavanpatil, M. D.; Patil, Y.; Panyam, J. Susceptibility of Nanoparticle-Encapsulated Paclitaxel to P-Glycoprotein-Mediated Drug Efflux. *Int. J. Pharm.* **2006**, *320*, 150-156.

(39) Xiao, L.; Xiong, X.; Sun, X.; Zhu, Y.; Yang, H.; Chen, H.; Gan, L.; Xu, H.; Yang, X. Role of Cellular Uptake in the Reversal of Multidrug Resistance by PEG-*b*-PLA Polymeric Micelles. *Biomaterials* **2011**, *32*, 5148-5157.

(40) Cho, Y. W.; Lee, J.; Lee, S. C.; Huh, K. M.; Park, K. Hydrotropic Agents for Study of in Vitro Paclitaxel Release from Polymeric Micelles. *J. Controlled Release* **2004**, *97*, 249-257.

(41) Satoh, K.; Poelma, J. E.; Campos, L. M.; Stahl, B.; Hawker, C. J. A Facile Synthesis of Clickable and Acid-Cleavable PEO for Acid-Degradable Block Copolymers. *Polym. Chem.* **2012**, *3*, 1890-1898.

(42) Wang, J.; Mao, W.; Lock, L. L.; Tang, J.; Sui, M.; Sun, W.; Cui, H.; Xu, D.; Shen, Y. The Role of Micelle Size in Tumor Accumulation, Penetration, and Treatment. *ACS Nano* **2015**, *9*, 7195-7206.

(43) Choi, J. S.; Cao, J.; Naeem, M.; Noh, J.; Hasan, N.; Choi, H. K.; Yoo, J. W. Size-Controlled Biodegradable Nanoparticles: Preparation and Size-Dependent Cellular Uptake and Tumor Cell Growth Inhibition. *Colloid. Surface B.* **2014**, *122*, 545-551.

(44) Huo, M.; Zou, A.; Yao, C.; Zhan, Y.; Zhou, J.; Wang, J.; Zhu, Q.; Li, J.; Zhang, Q. Somatostatin Receptor-Mediated Tumor-Targeting Drug Delivery using Octreotide-PEG-

Deoxycholic Acid Conjugate-Modified N-deoxycholic Acid-O, N-hydroxyethylation Chitosan Micelles. *Biomaterials* **2012**, *33*, 6393-6407.

(45) Zheng, S.; Jin, Z.; Han, J.; Cho, S.; Ko, S. Y.; Park, J. O.; Park, S. Preparation of HIFU-Triggered Tumor-Targeted Hyaluronic Acid Micelles for Controlled Drug Release and Enhanced Cellular Uptake. *Colloids Surf., B.* **2016**, *143*, 27-36.

(46) Chithrani, B. D.; Ghazani, A. A.; Chan, W. C.. Determining the Size and Shape Dependence of Gold Nanoparticle Uptake into Mammalian Cells. *Nano lett* **2006**, *6*, 662-668.

(47) Amin, M. L.; Kim, D.; Kim, S.. Development of Hematin Conjugated PLGA Nanoparticle for Selective Cancer Targeting. *Eur. J. Pharm. Sci*. **2016**, *91*, 138-143.

(48) Wu, H.; Zhu, L.; Torchilin, V. P. pH-Sensitive Poly (histidine)-PEG/DSPE-PEG Co-Polymer Micelles for Cytosolic Drug Delivery. *Biomaterials* **2013**, *34*, 1213-1222.

(49) Belotti, D.; Vergani, V.; Drudis, T.; Borsotti, P.; Pitelli, M. R.; Viale, G.; Giavazzi, R.; Taraboletti, G. The Microtubule-Affecting Drug Paclitaxel Has Antiangiogenic Activity. *Clin. Cancer Res.* **1996**, *2*, 1843-1849.

(50) Choi, J.; Konno, T.; Takai, M.; Ishihara, K. Regulation of Cell Proliferation by Multi-Layered Phospholipid Polymer Hydrogel Coatings Through Controlled Release of Paclitaxel. *Biomaterials* **2012**, *33*, 954-961.

(51) Assanhou, A. G.; Li, W.; Zhang, L.; Xue, L.; Kong, L.; Sun, H.; Mo, R.; Zhang, C. Reversal of Multidrug Resistance by Co-Delivery of Paclitaxel and Lonidamine Using a TPGS and Hyaluronic Acid Dual-Functionalized Liposome for Cancer Treatment. *Biomaterials* **2015**, *73*, 284-295.

(52) Yim, H.; Park, W.; Kim, D.; Fahmy, T. M.; Na, K. A Self-Assembled Polymeric Micellar Immunomodulator for Cancer Treatment Based on Cationic Amphiphilic Polymers. *Biomaterials* **2014**, *35*, 9912-9919.

(53) Zhu, Y.; Zhang, J.; Meng, F.; Deng, C.; Cheng, R.; Feijen, J.; Zhong, Z. cRGD-Functionalized Reduction-Sensitive Shell-Sheddable Biodegradable Micelles Mediate Enhanced Doxorubicin Delivery to Human Glioma Xenografts in Vivo. *J. Controlled Release* **2016**, *233*, 29-38.

(54) Zhu, Y.; Wang, X.; Zhang, J.; Meng, F.; Deng, C.; Cheng, R.; Feijen, J.; Zhong, Z. Exogenous Vitamin C Boosts the Antitumor Efficacy of Paclitaxel Containing Reduction-Sensitive Shell-Sheddable Micelles in Vivo. *J. Controlled Release* **2017**, *250*, 9-19.

pH-Responsive Poly(Ethylene Glycol)-*block*-Polylactide Micelles for Tumor-Targeted Drug Delivery

Lin Xiao, [†,‡] *Lixia Huang,* [†,‡] *Firmin Moingeon,* [§] *Mario Gauthier,* [§,*] *Guang Yang*[†,*]

[†] Department of Biomedical Engineering, College of Life Science and Technology, Huazhong University of Science and Technology, Wuhan 430074, China.

[§] Department of Chemistry, University of Waterloo, Waterloo N2L 3G1, Canada.

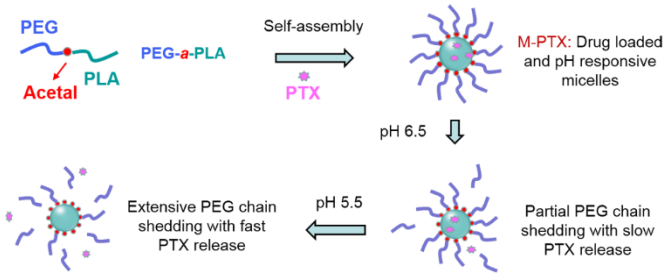

For Table of Contents Use Only